

# **SLOSHING IN THE LIQUID HYDROGEN AND LIQUID OXYGEN PROPELLANT TANKS AFTER MAIN ENGINE CUT OFF**

Sura Kim  
MSFC/ER42-Jacobs  
CFD Research Corp.  
Huntsville, AL

Jeff West  
NASA/MSFC ER42  
MSFC, AL

## **ABSTRACT**

NASA Marshall Space Flight Center is designing and developing the Main Propulsion System (MPS) for Ares launch vehicles. Propellant sloshing in the liquid hydrogen (LH<sub>2</sub>) and liquid oxygen (LO<sub>2</sub>) propellant tanks after Main Engine Cut Off (MECO) was modeled using the Volume of Fluid (VOF) module of the computational fluid dynamics code, CFD-ACE+. The present simulation shows that there is substantial sloshing side forces acting on the LH<sub>2</sub> tank during the deceleration of the vehicle after MECO. The LH<sub>2</sub> tank features a side wall drain pipe. The side loads result from the residual propellant mass motion in the LH<sub>2</sub> tank which is initiated by the stop of flow into the drain pipe at MECO. The simulations show that radial force on the LH<sub>2</sub> tank wall is less than 50 lbf and the radial moment calculated based up through the center of gravity of the vehicle is predicted to be as high as 300 lbf-ft. The LO<sub>2</sub> tank features a bottom dome drain system and is equipped with sloshing baffles. The remaining LO<sub>2</sub> in the tank slowly forms a liquid column along the centerline of tank under the zero gravity environments. The radial force on the LO<sub>2</sub> tank wall is predicted to be less than 100 lbf. The radial moment calculated based on the center of gravity of the vehicle is predicted as high as 4500 lbf-ft just before MECO and dropped down to near zero after propellant draining stopped completely.

## **INTRODUCTION**

NASA Marshall Space Flight Center is designing and developing the Main Propulsion System (MPS) for Ares launch vehicles. Propellant sloshing under large body forces either from gravitational or flight accelerations can be modeled with traditional approaches using a mass-spring-damper model. When the body force becomes small as gravity or acceleration forces vanish, the mass-spring-damper model is no longer valid. Under these conditions the liquid surface tension takes on the dominant role in the static or dynamic behavior of the liquid. CFD analysis offers an important tool to analyze the liquid movement and the resulting sloshing forces and moments which are the critical quantities in the modeling control and stability of the vehicle.

The objective of this study is to calculate the sloshing forces and moments in the LH<sub>2</sub> and LO<sub>2</sub> propellant tanks using a CFD/VOF analysis under realistic flight conditions. Liquid draining and motion was first modeled for both Hydrogen and Oxygen tank liquids for the time from first stage engine ignition to MECO by ER42, MSFC [1]. The simulations were then continued using the restart file from a condition just before MECO and continuing for 30 seconds during non-propulsive coasting.

## **ANALYSIS APPROACH**

### **FLUID ANALYSIS**

The computational multi-physics code, CFD-ACE+, is used to predict the liquid sloshing behavior in a propellant tank. CFD-ACE+ comprises of a set of modules for multi-physics computational analyses [2]. The modules include an integrated geometry and grid generation module, a graphical user interface for

preparing the model, and a computational solver for performing the simulations. The numerical solution yields discrete field values of the variables at the cell centers. The Partial Differential Equations (PDE's) governing the physics can be expressed in the form of a generalized transport equation. The numerical approach to solve these PDE's consists of the discretization of the PDE's on a computational grid, the formation of a set of algebraic equations, and the solution of the algebraic equations. In the finite volume approach of CFD-ACE+, the governing equations are numerically integrated over each of these computational cells or control volumes. There are several modules of CFD-ACE+ that are tightly coupled with the flow solver. The modules used to perform the current analyses included fluid flow Navier-Stokes solver and the VOF module. The flow module uses a SIMPLEC or PISO algorithm to sequentially solve the incompressible or compressible Navier-Stokes equations using either structured, unstructured, or hybrid computational meshes with finite volume integration.

Since the study includes two fluids, gas and liquid, the VOF equation described below is solved together with the fundamental equations of conservation of mass and momentum and energy when activated in CFD-ACE+ to achieve computational coupling between the velocity field solution and the liquid distribution. The characterizing feature of the VOF methodology is that the distribution of the second fluid in the computational grid is accounted for using a single scalar field variable,  $F$ , that specifies the fraction of the volume of each computational cell in the grid occupied by liquid. Thus,  $F$  takes the value 1 in cells that contain only liquid and the value 0 in cells that contain only gas. A cell that contains an interface would have a value of  $F$  between 0 and 1. Given a flow field and an initial distribution of  $F$  on a grid, the manner in which the volume fraction distribution  $F$  and hence the distribution of liquid involved is determined by solving the passive transport equation

$$\frac{\partial F}{\partial t} + \nabla \bullet \vec{V}F = 0 \quad (1)$$

where  $F$  is the liquid volume fraction,  $t$  is time,  $\nabla$  is the standard spatial grad operator, and  $\vec{V}$  is the velocity vector. To compute mixture properties in the VOF calculation, the fluid-fluid interface in each cell needs to be reconstructed. An upwind scheme with the Piecewise Linear Interface Construction method (PLIC) for the surface reconstruction is adopted in the simulation. In CFD-ACE+, the PLIC-based VOF capability is only available in conjunction with a hexagonal structured mesh.

Since the surface advection calculation is explicit and has an inherent stability limit on the allowable time step magnitude, the size of time step for gas-liquid mixed cells must be restricted to ensure that the free surface crosses less than a single cell during each time step. This can be accomplished automatically in CFD-ACE+ by using the automatic time step option that controls the Courant condition in the entire simulation.

#### NATURAL FREQUENCY CALCULATION USING CFD-ACE+

The natural frequency of sloshing in a tank is calculated by monitoring the liquid mass oscillations from the CFD simulation. Since we are not dealing with a point mass, we need to find the equation of motion or Newton's second law of motion for the center of mass of the liquid inside the tank. The center of mass is defined as

$$\vec{r}_c = \frac{1}{M} \int \vec{r} dm \quad (2)$$

where  $M$  is the mass of the liquid inside the tank. The mass  $M$  is equal to the product of the density of liquid, denoted here as  $\rho$  and the volume of liquid in the tank,  $M = \rho V_{\text{liquid}}$ . The center of mass of the liquid oscillates about its equilibrium position with an angular frequency,  $\omega_0$ , as shown in figure 1. The frequency of oscillation is equal to

$$f = \frac{\omega_0}{2\pi} \quad (3)$$

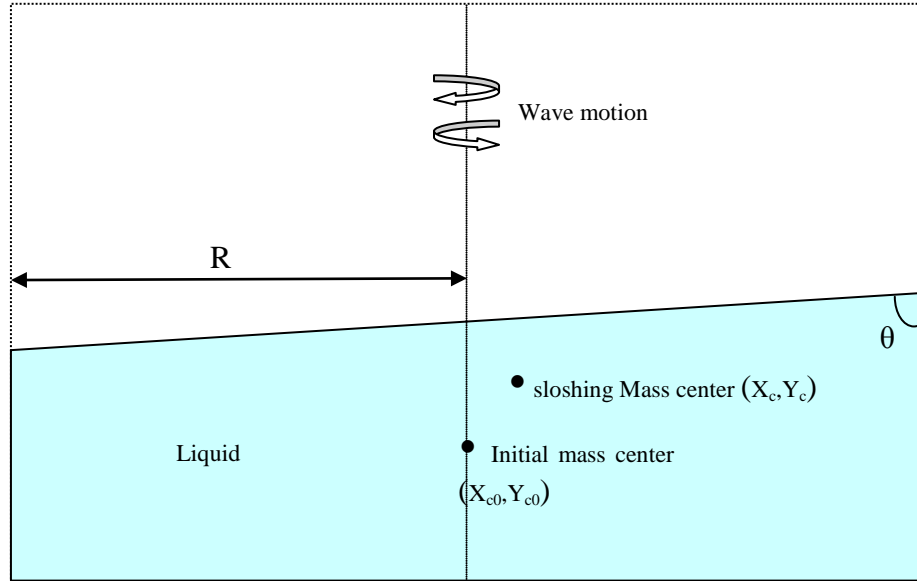


Figure 1. Schematic of mass sloshing.

The above was coded in a user subroutine that was used by CFD-ACE+ for natural frequency calculations. The theoretical natural frequency of a cylinder with an ellipsoidal bottom is predicted at 0.00017 Hz [4, 5]. However, because the duration of simulation is only 30 second, the calculation is not expected to capture this low frequency.

#### INCORPORATION OF EXTERNAL BODY FORCE FOR NON-INERTIAL FRAME.

Newton's law of  $\vec{f} = \vec{m}\vec{a}$  is manipulated for the non-inertial frame as follows. The first term of the last line in figure 2 indicates the center of gravity, the third term the Coriolis acceleration, the forth term the angular acceleration, and the last term the centrifugal acceleration. These quantities are incorporated into the main solver through a user subroutine.

in: inertial frame, r: rotating frame

$$\begin{aligned} \left(\frac{d\vec{A}}{dt}\right)_{in} &= \left(\frac{d\vec{A}}{dt}\right)_r + \vec{\omega} \times \vec{A} \\ \text{let } \vec{r}' &= \vec{R} + \vec{r}, \\ \left(\frac{d\vec{r}'}{dt}\right)_{in} &= \left(\frac{d\vec{R}}{dt}\right)_{in} + \left(\frac{d\vec{r}}{dt}\right)_{in} = \vec{v}_{cg} + \vec{v}_r + \vec{\omega} \times \vec{r} \\ \text{let } \vec{a}_{in} &= \frac{d}{dt} \left(\frac{d\vec{r}'}{dt}\right)_{in}, \vec{a}_r = \left(\frac{d\vec{v}_r}{dt}\right)_r, \text{then} \\ \vec{a}_{in} &= \left(\frac{d\vec{v}_{cg}}{dt}\right)_{in} + \left(\frac{d\vec{v}_r}{dt}\right)_{in} + \left(\frac{d\vec{\omega}}{dt}\right)_{in} \times \vec{r} + \vec{\omega} \times \left(\frac{d\vec{r}}{dt}\right)_{in} \\ &= \vec{a}_{cg} + (\vec{a}_r + \vec{\omega} \times \vec{v}_r) + \dot{\vec{\omega}} \times \vec{r} + \vec{\omega} \times (\vec{v}_r + \vec{\omega} \times \vec{r}) \\ &= \vec{a}_{cg} + \vec{a}_r + 2\vec{\omega} \times \vec{v}_r + \dot{\vec{\omega}} \times \vec{r} + \vec{\omega} \times (\vec{\omega} \times \vec{r}) \end{aligned}$$

*Figure 2. Newton's law for the non-inertial frame.*

## GEOMETRY AND MODEL SETUP

### GEOMETRY OF LIQUID HYDROGEN TANK

The hexagonal structured grid systems for the both tanks were generated using the CFD-GEOM grid generation tool [2]. Figure 3 presents the grid system of hydrogen tank. The tank features smooth internal walls without baffles. The total number of cells is 940,848.

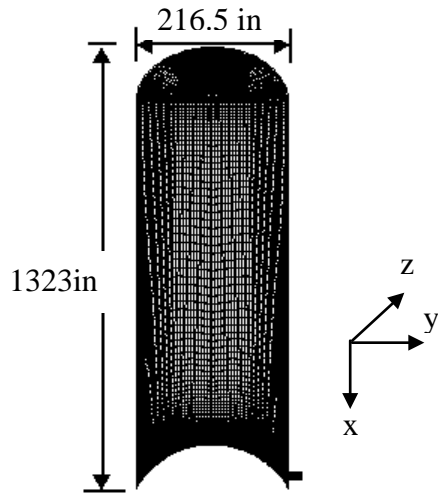


*Figure 3. Hydrogen tank geometry.*

### GEOMETRY OF LIQUID OXYGEN TANK

Figure 4 presents the grid system of liquid oxygen tank. Notice that the tank features internal sloshing baffles. The total number of cells is 201,540 cells.

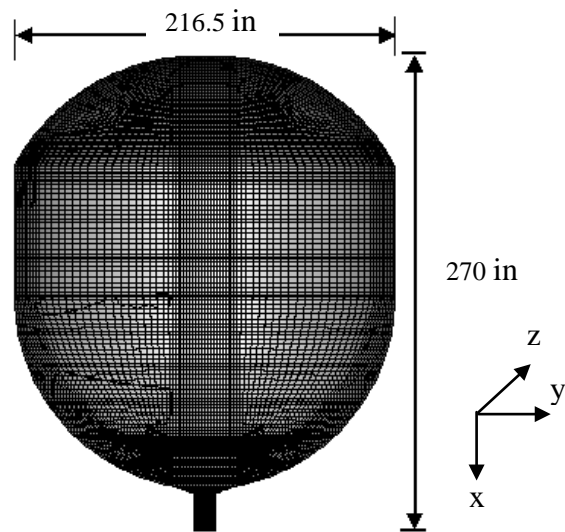


*Figure 4. Oxygen tank geometry.*

## MODEL SET-UP FOR LIQUID HYDROGEN AND OXYGEN TANKS

Although the flow is turbulent at the exit tube, the flow in the tank is assumed a transient, laminar, and incompressible flow. The VOF module of CFD-ACE+ has several simulation control options. Since the surface advection calculation is explicit and has an inherent stability limit on the allowable time step magnitude, the time step size for the gas-liquid mixed cells must be restricted to ensure that the free surface crosses less than a cell during that time step. This can be accomplished by selecting the "auto time step" option that controls the Courant condition in the entire simulation. Upon using auto time step, the Fast Time Stepping (FTS) option internally switches the solver algorithm from Semi-Implicit Method for Pressure Linked Equations (SIMPLE) to Pressure Implicit Splitting of Operators (PISO) to enhance the convergence. Also the FTS option currently supports only the first order accurate in time. This report contains simulation results generated with an Euler scheme for time advancing and an upwind method for spatial differencing that proved to be more stable. The surface reconstruction method namely PLIC was adopted. PLIC is a second order interface reconstruction scheme. In the simulation, we applied the structured grid system due to the PLIC method limitation and PISO algorithm to use the FTS option for the flow solver.

The Conjugate Gradient Squared (CGS) solver algorithm was used as the solver for the velocity and pressure correction equations. The convergence criterion was set to 1e-4. The user subroutine was executed for: (1) the calculation of the natural frequency, (2) incorporation of external body forces (gravity and vehicle accelerations) in the non-inertial frame.

## ESTIMATION OF CONTACT ANGLE BETWEEN PROPELLANTS AND TANK WALL

Pictures taken from the inside of the liquid hydrogen tank of the Saturn AS-203 and the inside of liquid oxygen tank of the Saturn SA-5 are available. Snapshots were taken from DVD movie footage and used to determine the actual contact angles of the propellants. Results are presented in Figure 5 and Appendix A.

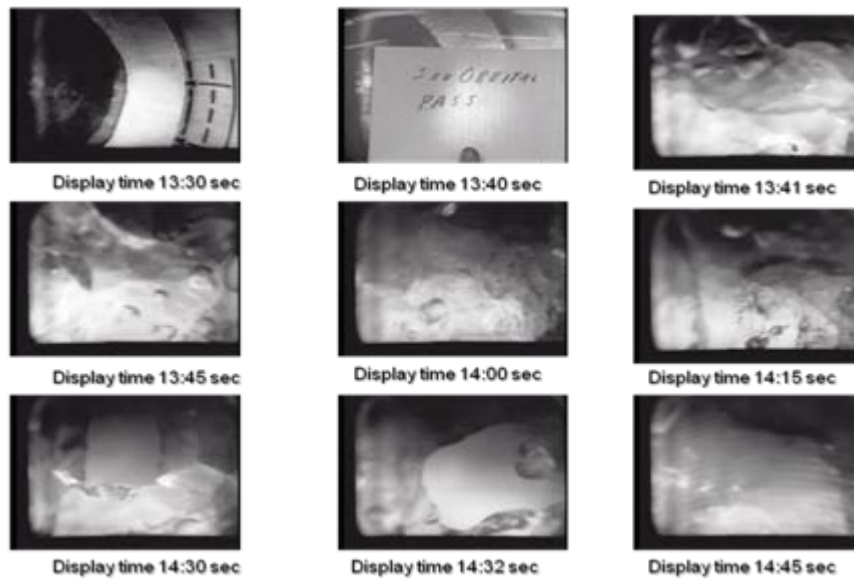


Figure 5. Pictures taken from the inside the liquid hydrogen tank of Saturn AS-203

It was not possible to positively determine the contact angle from the pictures. However, the contact angle between liquid hydrogen and the wall was observed to clearly be larger than zero degrees, unlike the zero contact angle typically found between water and a wall. The contact angle of the liquid hydrogen was estimated to be 30 degrees and that of the liquid oxygen to be 5 degrees. These values are used in the subsequent calculations.

## FLIGHT INPUT CONDITIONS

Estimated flight conditions of ARES-1 [3] are applied to the liquid mass sloshing simulations through the body forces user subroutine as stated in Section 2.3. Figures 6a through 6c present the input body forces for the simulations. Figure 7 presents the propellant flow rate schedule of ARES-1. The flow rates are converted to velocities and applied as the tank exit flow velocity boundary condition.

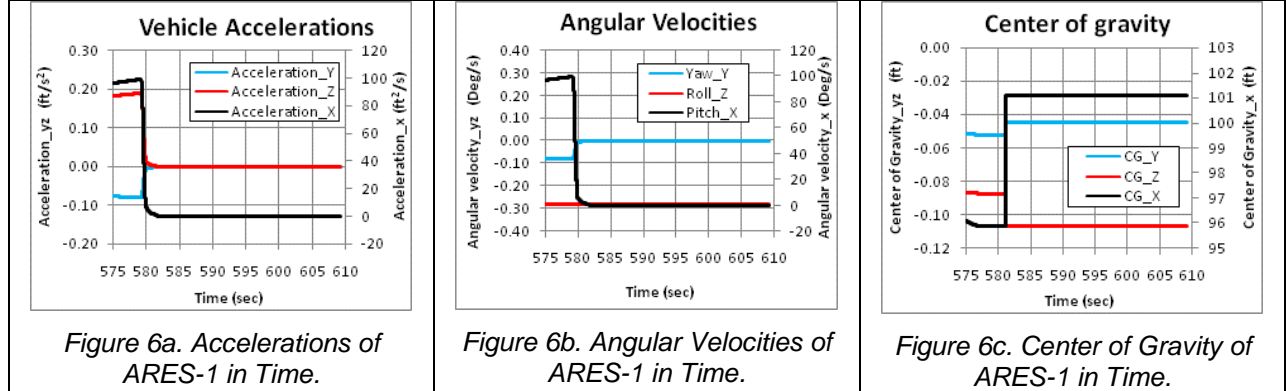


Figure 6a. Accelerations of ARES-1 in Time.

Figure 6b. Angular Velocities of ARES-1 in Time.

Figure 6c. Center of Gravity of ARES-1 in Time.

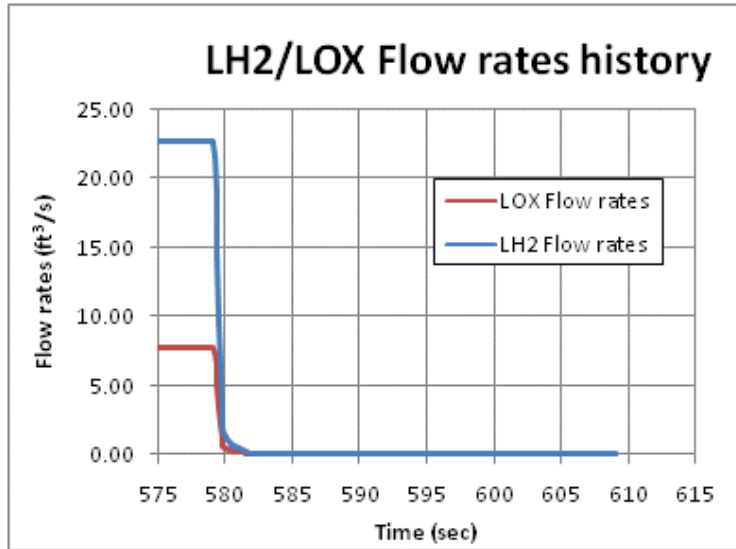
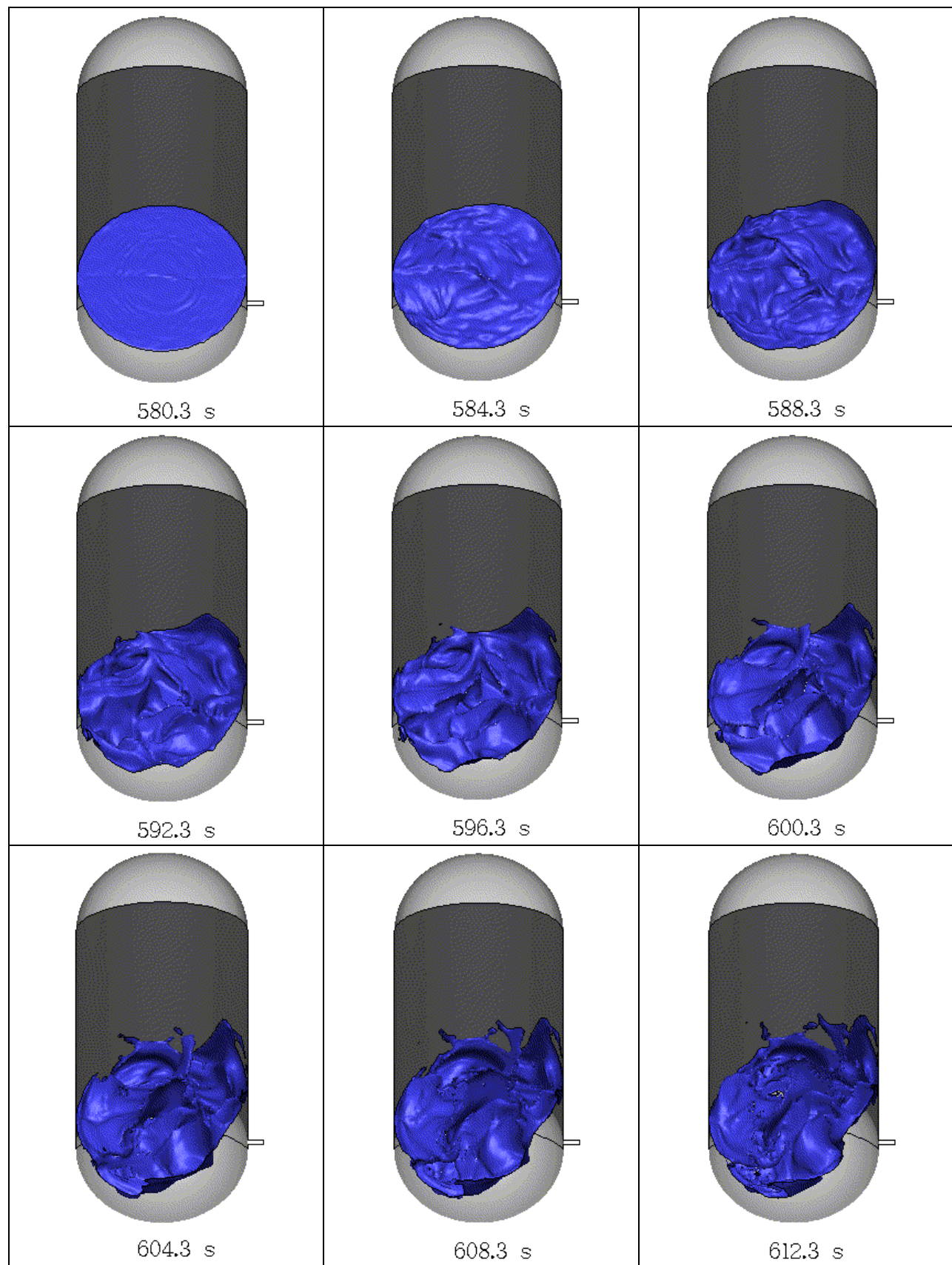


Figure 7. LH2/LO2 flow rates history of ARES 1.

## RESULTS AND DISCUSSIONS

### LIQUID HYDROGEN TANK

The simulation for the LH2 tank after MECO was performed with a restart file [1] from the 580.31 seconds conditions after lift-off. Tank pressure at the ullage space in the tank was maintained during the propellant drain process by assuming an open top boundary condition with fixed pressure. Figure 8 shows the snapshot plots of the history of the liquid-gas interface for the hydrogen sloshing after MECO under microgravity environments. Note that the interface on the right hand side of the Figures moves higher than the left hand side. The tank drain pipe is located on the right side. The pressure at the right hand side is temporarily higher than the left hand side as a result of the sudden stop of LH2 flow in the drain pipe region at 581.9 seconds.



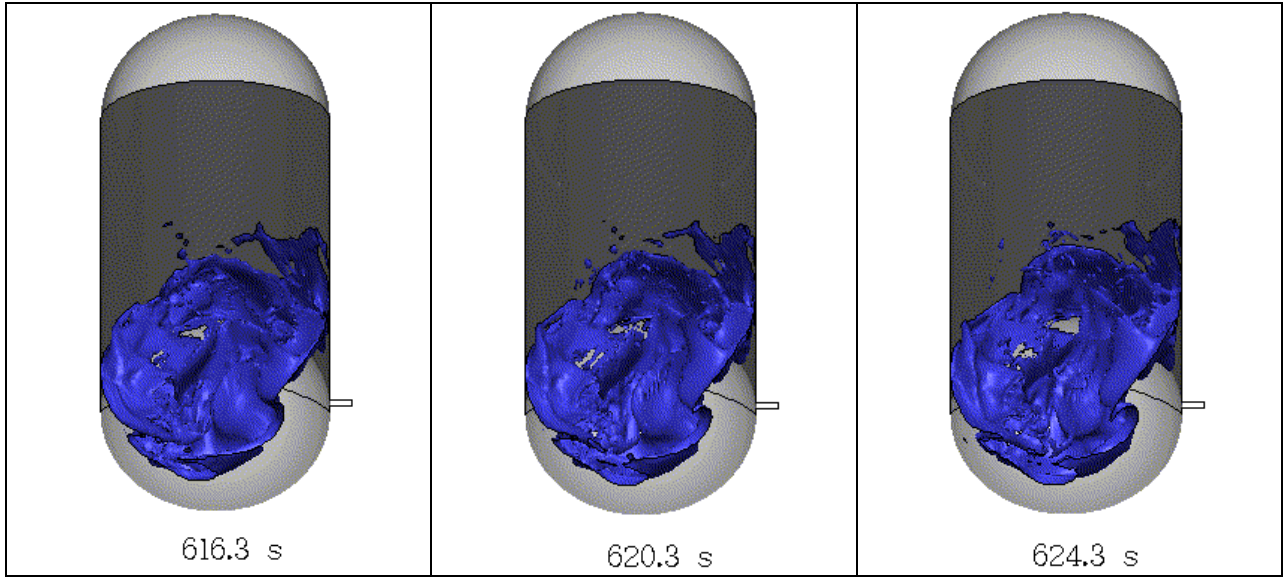


Figure 8. Changes of the gas-liquid interface under the micro gravity environments.

Figures 9a to 9c present the time history of the LH<sub>2</sub> liquid mass center positions. The curves indicate that the natural frequency is extremely low. The theoretical natural frequency of a cylinder with an ellipsoidal bottom is predicted at 0.00017 Hz [4, 5]. Because the duration of simulation is only 30 second, the calculation was not expected to capture this low frequency.

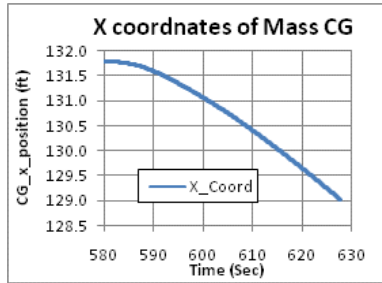


Figure 9a. History of mass-center position in X vs. Time

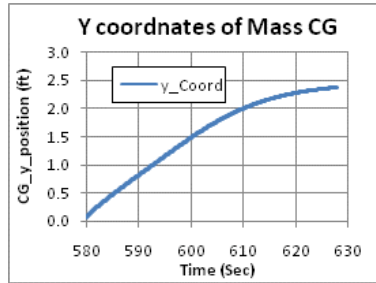


Figure 9b. History of mass-center position in Y vs. Time

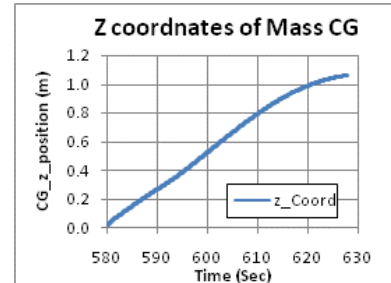


Figure 9c. History of mass-center position in Z vs. Time

Figures 10a to 10c show the forces acting on the x, y, and z directional walls. Figures also include curve fits derived for the force curves. These curve fit formulas are:

$$\begin{aligned} \text{X axial force} &= 1800 * \text{EXP}(-1.7 * (\text{time} - 580.03)) \text{ [lbf]} \\ \text{Y radial force} &= 10 * \text{EXP}(-2.2 * (\text{time} - 580.03)) \text{ [lbf]} \\ \text{Z radial force} &= 8 * \text{EXP}(-1.5 * (\text{time} - 580.03)) \text{ [lbf]} \end{aligned}$$

Note that the mass of the liquid hydrogen remaining in the tank at the time of MECO is 4541 lbm and the cross sectional area of the tank is 23.76 m<sup>2</sup> (255 ft<sup>2</sup>). In Figure 10a, a positive axial force means that the force is acting in the direction towards the bottom of the tank.

The axial force is initially predicted over 7100 lbf at about 579 seconds and continuously drops near zero as the propellant draining stopped. Note that the force acting on the dome surface that is assumed as the outlet boundary during the simulation is estimated at less than 20 lbf. Radial force (Figure 10b and 10c) is predicted less than 50 lbf. Figures 11a to 11c show the moments of the tank in x, y, and z direction, respectively. Moments are calculated based up the center of gravity of the vehicle. Radial moment is

predicted as high as 300 lbf-ft. Figures 12a to 12c show the pressure gradient in the tank. While propellant is in draining process, pressure gradient in the tank is about 0.04 psi during. (Figure 12a) But the pressure gradient in the tank disappears when the propulsion acceleration ceases (Figure 12c).

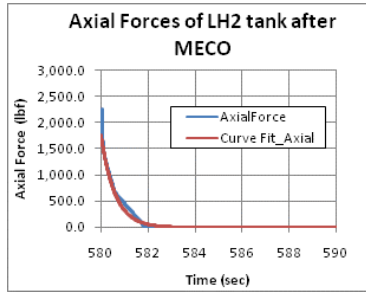


Figure 10a. Forces in axial direction

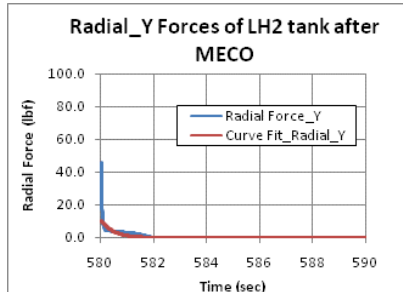


Figure 10b. Forces in Y radial direction

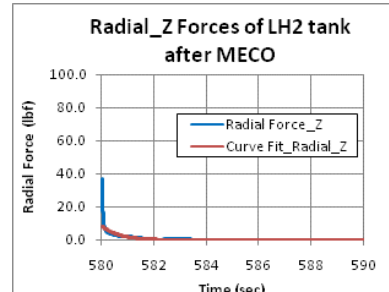


Figure 10c. Forces in Z radial direction

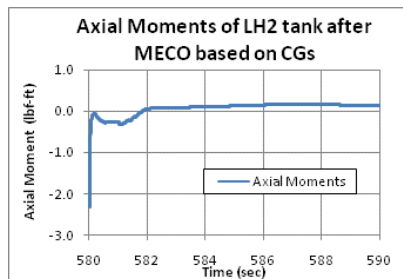


Figure 11a. Moments in axial direction

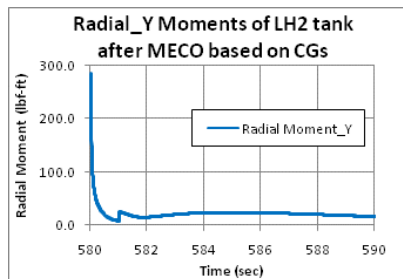


Figure 11b. Moments in Y radial direction

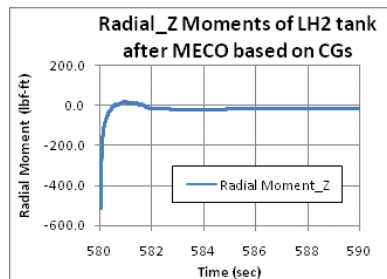


Figure 11c. Moments in Z radial direction

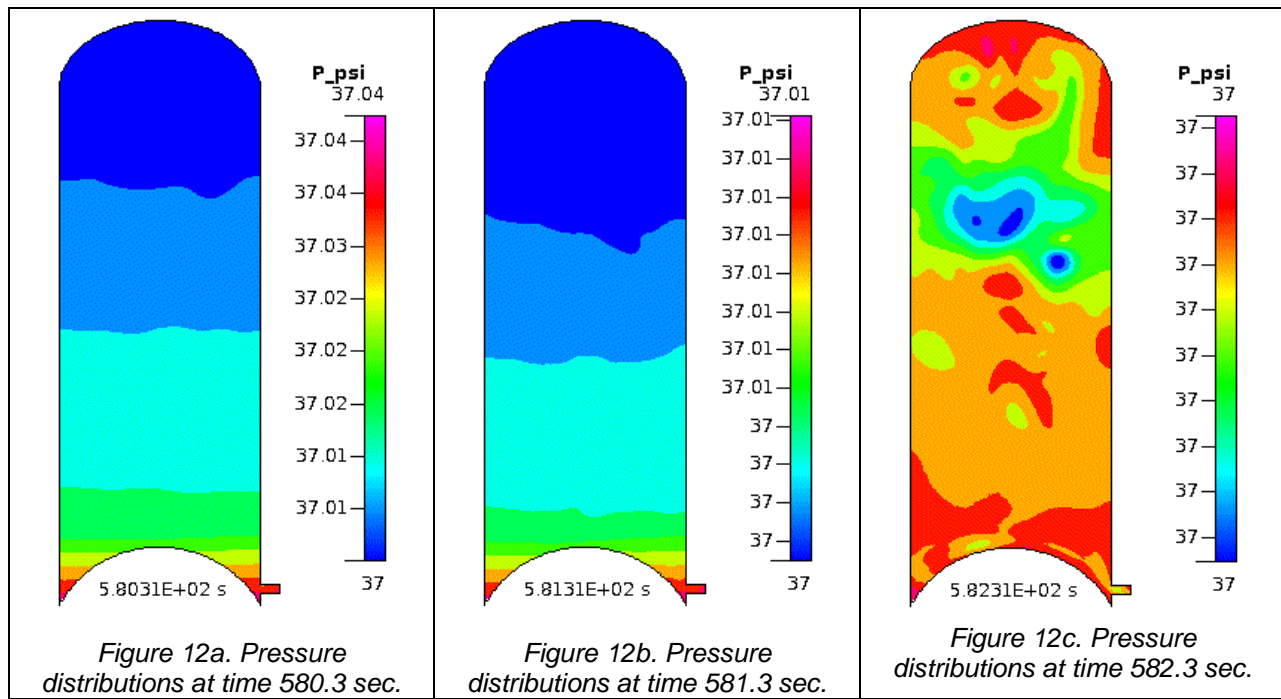


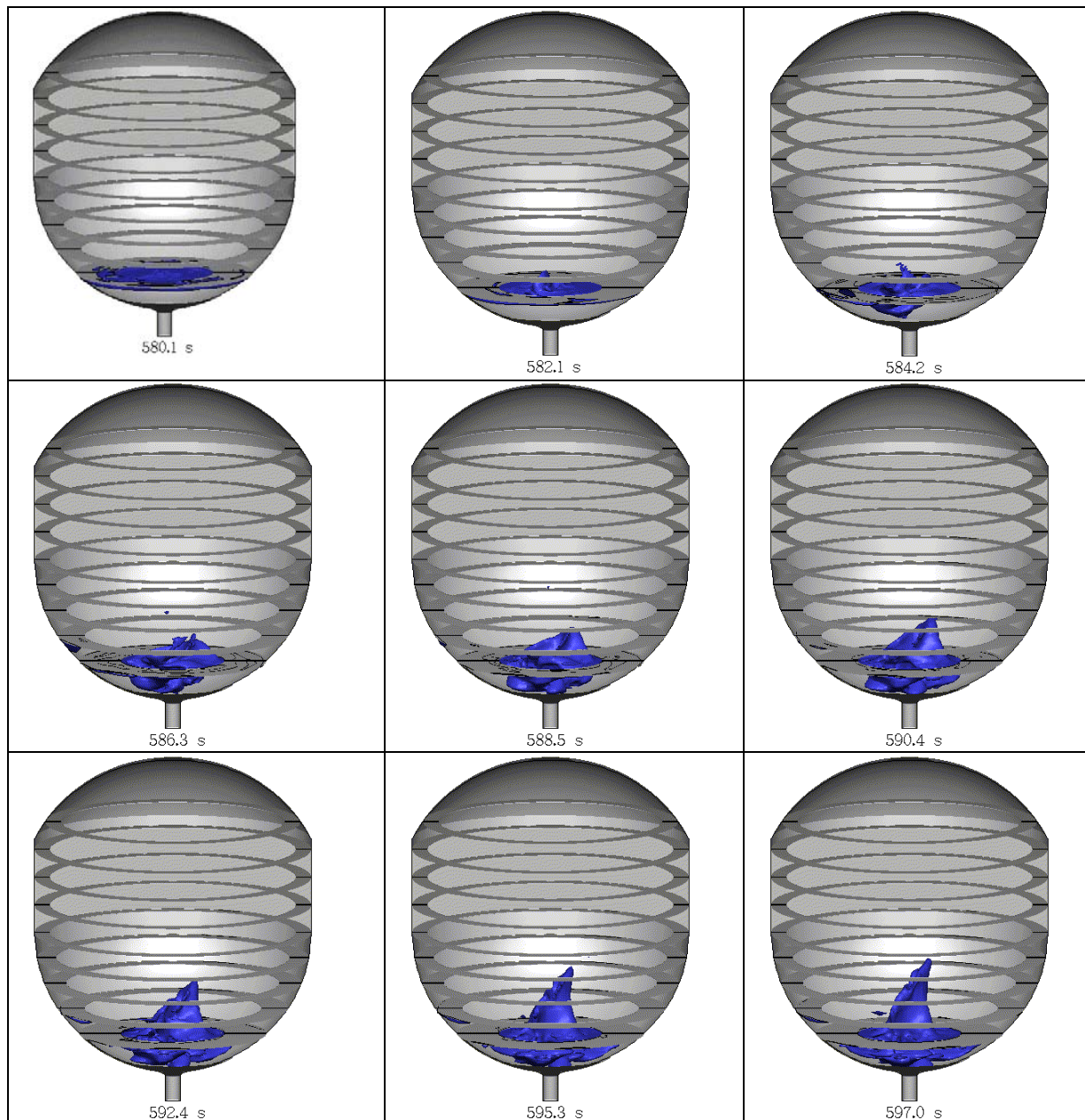
Figure 12a. Pressure distributions at time 580.3 sec.

Figure 12b. Pressure distributions at time 581.3 sec.

Figure 12c. Pressure distributions at time 582.3 sec.

## LIQUID OXYGEN TANK

The simulation for the LO<sub>2</sub> tank after MECO was performed with a restart file [2] from the 590.3 seconds conditions after vehicle lift-off. Tank pressure at ullage space in the tank was maintained during the propellant drain process by assuming the outlet boundary condition at the top of the tank. In the LO<sub>2</sub> tank simulation, the amount of LO<sub>2</sub> remaining after MECO is approximately 62.3 ft<sup>3</sup> by volume and its liquid level is 30.3 inch above the entrance of the LO<sub>2</sub> exit tube. Figure 13 shows snapshot plots of the liquid-gas interface. The remaining liquid in the tank slowly forms a liquid column as shown in figure 13. This is because the propellant was drained during draining process and was stopped after MECO from the bottom center of the tank. As a results, the high pressure, built up from the inside of the exit pipe due to stop the propellant draining, propagates upward and pushes the gas-liquid interface upward along the centerline of the tank (figure 14).



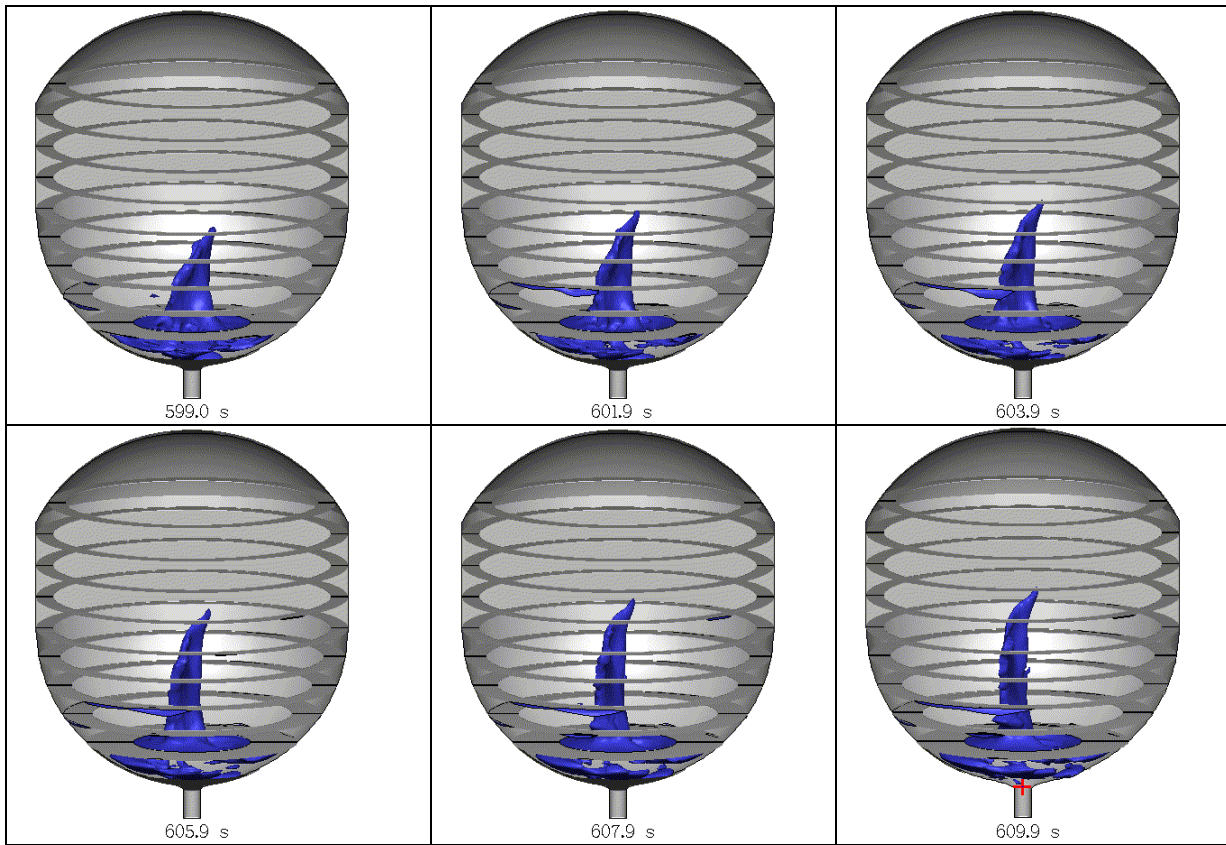


Figure 13. Plots of the gas-liquid interface (3D simulation).

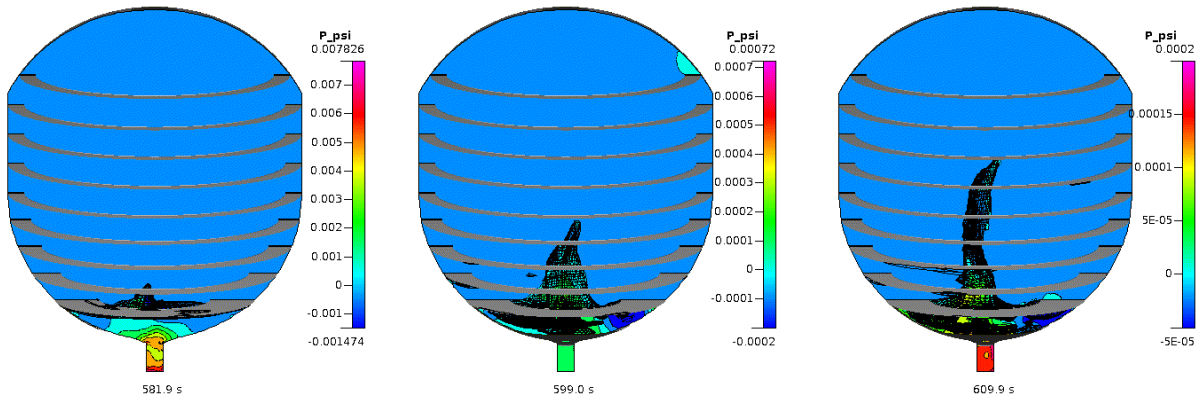


Figure 14. The gas-liquid interface and pressure distribution along the center cut of the tank.

Figures 15a to 15c show the forces acting on the x, y, and z directional walls. Figures also include the curve fit of the forces. These formulas are:

$$\begin{aligned}
 \text{X axial force} &= 6500 * \text{EXP}(-1.5 * (\text{time} - 579.03)) \text{ [lbf]} \\
 \text{Y radial force} &= 450 * \text{EXP}(-1.5 * (\text{time} - 579.03)) \text{ [lbf]} \\
 \text{Z radial force} &= 300 * \text{EXP}(-1.4 * (\text{time} - 579.03)) \text{ [lbf]}
 \end{aligned}$$

Note that the mass of the liquid oxygen remaining in the tank at the time of MECO is approximately 9420 lbm and the cross sectional area of the tank is  $23.76 \text{ m}^2$  ( $255 \text{ ft}^2$ ). In Figure 15a, the positive axial force indicates that the force is acting in the direction towards the bottom of the tank. The axial force is initially approximately 6500 lbs at 579.03 seconds and drops down to near zero after liquid draining stopped

(MECO). Note that the force acting on the dome surface is near zero. Radial force (Figure 15b and 15c) is predicted less than 100 lbf. Figures 16a to 16c show moments of the oxygen tank in x, y, and z direction, respectively. Radial moment calculated based up the center of gravity of the vehicle is predicted as high as 4500 lbf-ft just before MECO and dropped down to near zero after propellant draining stopped completely. As shown in Figures 17a to 17c, the pressure gradient in the tank is initially 5.6 psi during the propellant draining process (Figure 17a) and becomes within 0.017 psi when the propellant draining stopped (Figure 17c).

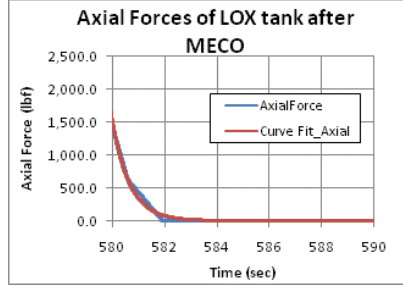


Figure 15a. Forces in axial direction.

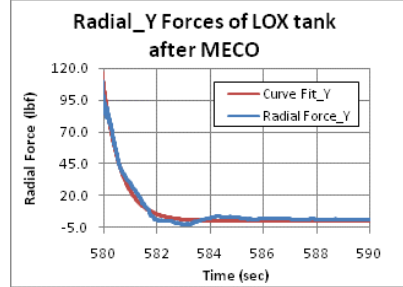


Figure 15b. Forces in Y radial direction.

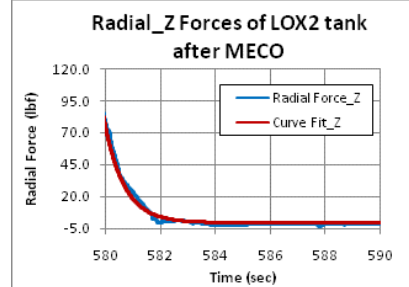


Figure 15c. Forces in Z radial direction.

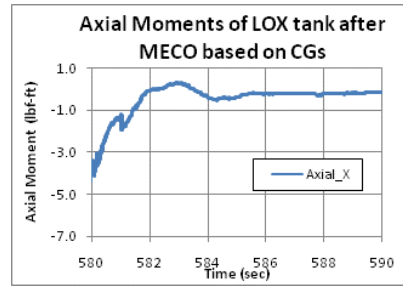


Figure 16a. Moments in axial direction

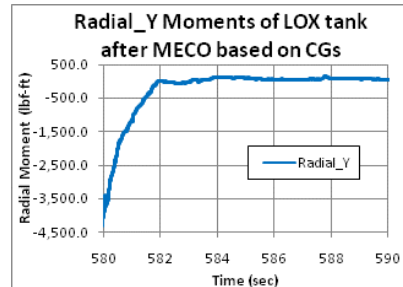


Figure 16b. Moments in Y radial direction

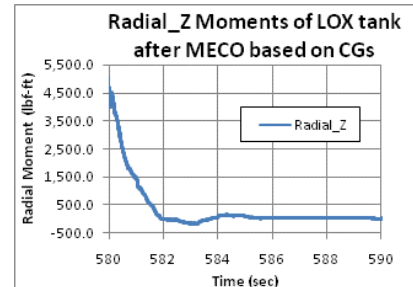


Figure 16c. Moments in Z radial direction

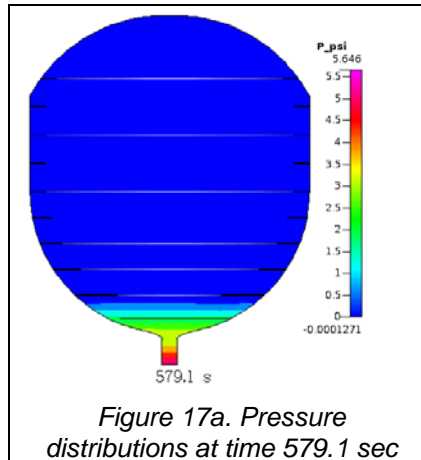


Figure 17a. Pressure distributions at time 579.1 sec

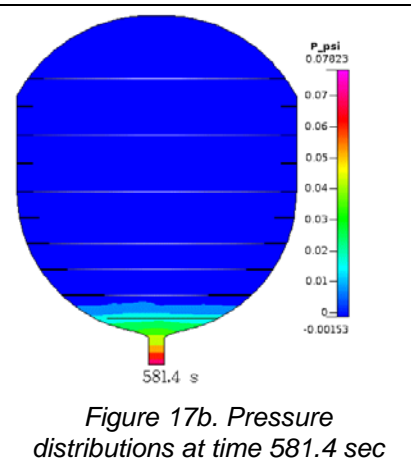


Figure 17b. Pressure distributions at time 581.4 sec

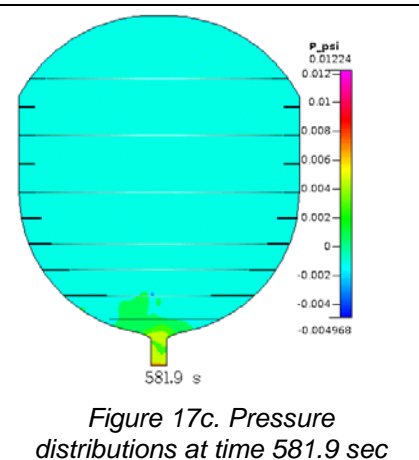


Figure 17c. Pressure distributions at time 581.9 sec

## SUMMARY AND CONCLUSIONS

Propellant sloshing under large body forces from gravitational or flight accelerations can be modeled with traditional approaches using a mass-spring-damper model. When the body force becomes small as gravity (micro gravity) or acceleration forces vanish such as in the after main engine shut off, the mass-spring-damper model becomes invalid. Under these conditions the liquid surface tension takes on the

dominant role in the static or dynamic behavior of the liquid. CFD analysis was used to analyze the liquid movement and the resulting sloshing forces and moments that are critical for accurately predicting the control and stability of the vehicle.

The purpose of this task was to provide propellant tank slosh forces and moments under the micro gravity conditions immediately following MECO. Propellant tank sloshing was simulated with the multi-phase VOF capability of the CFD-ACE+ CFD program. A user subroutine was developed and integrated into CFD simulations that 1) enforced prescribed vehicle trajectory forces and accelerations, and 2) extracted resulting propellant mass center of gravity (CG) location, and forces and moments acting on the tank walls during all phases of the vehicle flight.

Propellant flow simulations were carried out and saved for both LH<sub>2</sub> and LO<sub>2</sub> tanks from first stage ignition to just before MECO. Then, the last result files are used to the initial conditions of the subsequent micro-gravity analysis. The simulations were restarted under micro-gravity conditions for an additional 30 seconds beyond MECO and total forces and moments acting on the tank wall from the sloshing dynamics were extracted from the CFD simulations.

The present simulation showed that there are some substantial sloshing side forces acting on the LH<sub>2</sub> tank during the deceleration of the vehicle after MECO. The LH<sub>2</sub> tank features a side wall drain pipe. The side loads are results of the residual propellant mass motion in the LH<sub>2</sub> tank which is initiated by the stop of flow into the drain pipe as MECO. The simulations show that the frequency of propellant sloshing is very low as in the order of 2.0e-4 Hz. Radial force is predicted less than 50 lbf and radial moment calculated based up the center of gravity of the vehicle is predicted as high as 300 lbf-ft. The LO<sub>2</sub> tank features a bottom dome drain system and is equipped with sloshing baffles. The remaining liquid in the tank slowly forms a liquid column along the centerline of tank under the zero gravity environments. Radial force is predicted less than 100 lbf. Radial moment calculated based up the center of gravity of the vehicle is predicted as high as 4500 lbf-ft just before MECO and dropped down to near zero after propellant draining stopped completely.

## ACKNOWLEDGEMENTS

This project was funded by the NASA Marshall Space Flight Center under Jacobs ESTS Contract NNM05AB50C, Task Order 33-040218-CJ. This report documents the results of the study entitled "CFD Analyses of Liquid Hydrogen and Liquid Oxygen Tanks after Main Engine Cut Off (MECO)." Dr. Jeff West (MSFC Fluid Dynamics Branch, ER42) was the NASA Task Monitor and supported the project. Dr. Ramachandran, Narayanan R. was the Jacobs ESTS Group team lead Dr. Sura Kim of CFDRC was the principal investigator; Dr. H.Q. Yang who developed the user subroutine for the tank sloshing problem was the co-investigator.

## REFERENCES

- 1) Rojahn, Josh: "Propellant Sloshing in the Ares I Upper Stage Tanks from Lift-off to Main Engine Cut-Off", ESTSG-FY10-01191, Fluid Dynamic Branch, ER42, MSFC, 2010
- 2) CFD-ACE+ V.2003 User's Manual - Volume 2, 2004
- 3) TD-6F, Jon McDonald, ER22, MSFC, NASA, 2009
- 4) Jack A. Salzman and William J. Marsica: "Lateral Sloshing in Cylinders Under Low-Gravity Conditions," NASA TN D-5058, 1969
- 5) Franklin T. Dodge: "The New Dynamic Behavior of Liquids in Moving Containers," Southwest Research Institute, 2000.